

Perfusion Analysis for Lung MR Images Considering Non-Monotonic Response of Gd-Contrast Agent

Tomoki Saka ^{*,1} Masaki Ichikawa ^{*,2} Seiichiro Kagei ^{*,3}
Toshiyuki Gotoh ^{*,4} Tae Iwasawa ^{**,5}
Marcos de Sales Guerra Tsuzuki ^{***,6}

^{*} *Yokohama National University, 79-1 Tokiwadai, Hodogaya-ku,
Yokohama-shi, Kanagawa, 240-8501 Japan*

^{**} *Kanagawa Cardiovascular Respiratory Center, Kanazawa-ku,
Yokohama-shi, Kanagawa, 236-0051 Japan*

^{***} *Escola Politécnica da Universidade de São Paulo, Brazil.
Computational Geometry Laboratory*

Abstract: In order to remain in a monotonic concentration-signal relationship, tracer with low concentration is usually administrated. A new tracer concentration quantification to determine the non-monotonic effect and to enable the correct interpretation of the MR signal intensity, is proposed. It is based on the evaluation of the MR signal intensity in time that might have multiple peaks. A new method for perfusion analysis is also proposed, that is based on the blood flow inside the vessels like the γ variate model and the extravasation as the two compartment model. Samples of processing results of the proposed method applied to patients with confirmed cancer and pulmonary embolus are presented. *Copyright ©2014 IFAC.*

Keywords: Pulmonary blood flow, Gd contrast agent, Contrast agent permeation

1. INTRODUCTION

Perfusion scintigram has been a standard clinical tool for evaluating impaired perfusion. Recently, MR 4D imaging with gadolinium (Gd) contrast agent has been implemented in clinical and experimental studies (Berthezine et al., 1999). One main drawback is the fact that Gd contrast agent has a nonlinear and non-monotonic property; as Gd contrast agent concentration increases, the MR associated pixel intensity decreases.

Lung perfusion analysis is usually performed using the indicator dilution theory. Based on this theory, pulmonary perfusion parameters (blood flow, blood volume and mean transit time (MTT)) can be determined. It is assumed that the observed signal has one input and just one peak must be observed (Wang et al., 2013). For this reason, usually Gd contrast agent is used with relatively low concentration.

In this work it is proposed a new Gd contrast agent concentration quantification in which perfusion analysis can be performed with tracer higher concentration. Additionally, it is proposed a perfusion model based on the

two compartment model that considers permeation, an exchange of blood between vascular and extravascular volumes. The two compartment model is combined with the conventional γ fitting model. Considering the lung, two blood perfusion are present. One from the pulmonary system that oxygenates the blood, and the other from the systemic circulation that provides nutrients to the lung. A small percentage of the systemic blood flow goes to the lung and such blood flow keeps the lung with the necessary nutrients. Usually, such blood flow is ignored.

The proposed method considers just the first tracer concentration peak that reaches the lung after passing through the heart after injection. Such path corresponds to the pulmonary system perfusion. This work is structured as follows. Section 2 explains the proposed tracer concentration quantification. Section 3 explains some current methodologies used to evaluate the blood flow: indicator-dilution method and γ variate model. In this section, it is proposed a new model that combines the two compartment model with the γ variate model. Section 4 presents the materials and methods. Section 5 presents some results and the conclusions are in section 6.

2. TRACER CONCENTRATION QUANTIFICATION

Quantifying tracer concentration is essential to assess organ and tissue function. Although Gd has been used as a tracer material with MR, it is known that the tracer enhancement effect is not uniform for high concentrations of Gd. Usually, the quantification is done for each pixel of the lung through a linear relationship between the measured

¹ e-mail: sakachiki@gmail.com

² e-mail: ichikawa-masaki-nh@ynu.jp

³ e-mail: kagei@ynu.ac.jp

⁴ e-mail: gotoh@ynu.ac.jp

⁵ e-mail: tae.l.md@wb3.so-net.ne.jp

⁶ e-mail: mtsuzuki@usp.br. This author was partially supported by CNPq and FAPESP. This project was partially supported by a joint project from JSPS/CAPES and Grants-in-Aid for Scientific Research (24500539).

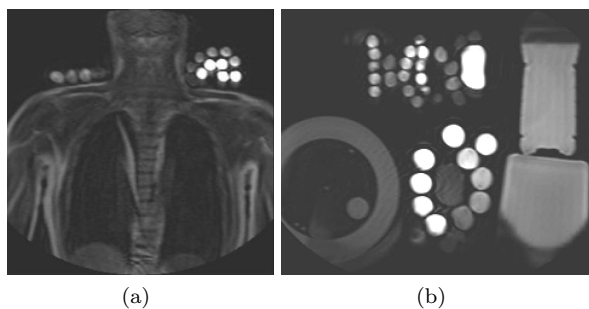


Fig. 1. (a) Phantoms with known tracer concentration obtained simultaneously with a patient chest MR image. (b) MR image exclusively with phantoms.

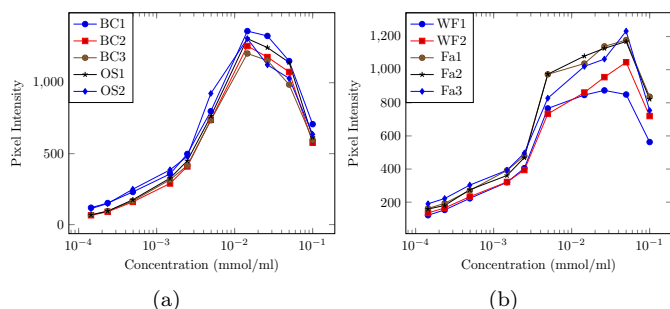


Fig. 2. (a) Graph of concentration \times pixel intensity with a subject. BC = Beside the Chest, OS = On Shoulders. (b) Graph of concentration \times pixel intensity without subjects. WF = Without Fat, Fa = With Fat.

MR signal and the tracer concentration. In order to remain in a reasonable concentration-signal relationship, usually low tracer concentration is administrated. However, in this case, the observation of capillary vessels is hampered due to signal weakness (Shahbazi-Gahrouei et al., 2001).

In this research, high concentrations of tracer are used to enable the observation of capillary vessels. Phantoms were used to map pixel intensity and tracer concentration. Considering Fig. 1(a), 10 phantoms were placed near the subject, in two different positions: beside the chest (3 cases) and on shoulders (2 cases). The results are summarized in Fig. 2(a), in which it is possible to conclude that the position has no influence in the imaging process.

In the following the influence of fat in the Gd enhanced imaging is evaluated (Low et al., 2002). Fig. 1(b) shows an image exclusively with phantoms, and it is desired to determine the influence of fat near the phantom. The large tube in the right of Fig. 1(b) has fat. The results are summarized in Fig. 2(b) and comparing both graphs, one might observe that they have different shapes. Based on this experiment, it was decided that the calibration must happen with phantoms and the subject within the same image.

The characteristic curve between tracer concentration and signal intensity has either negative and positive relationships, the following expression with two exponentials is used

$$S(x) = \lambda_a(e^{-\lambda_1 x} - e^{-\lambda_2 x}) + \lambda_b, \quad (1)$$

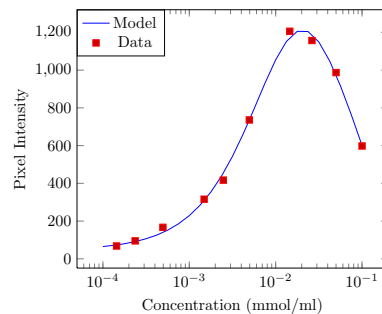


Fig. 3. Graph of concentration \times pixel intensity comparing acquired data and the determined model.

where λ_1 and λ_2 respectively represent the positive and negative relationships, λ_a and λ_b respectively are scale and offset parameters. The Levenberg-Marquardt algorithm is used to determine the parameters that minimizes the error in a least square fitting (Marquardt, 1963). Fig. 3 shows a calibrated curve obtained from an MR image with 10 samples. As (1) has four unknowns, it is necessary to have at least four phantoms with known tracer concentrations to determine the tracer concentration-MR signal intensity relationship. One of the phantoms must be of saline solution (with no tracer) and its concentration is considered as 0 mmol/ml.

Further investigation determined that for lower and higher tracer concentrations the efficacy is improved by shortening, respectively, T_1 and T_2 . T_1 is the spin-lattice relaxation time, and T_2 is the spin-spin relaxation time. As T_1 and T_2 have opposite relationship, by shortening T_1 and T_2 the respective parameters λ_1 and λ_2 can be determined with smaller errors (Rosen et al., 1990).

3. PERFUSION ANALYSIS

In this section, the indicator dilution method and the γ variate model are presented. It is also presented the proposed perfusion model.

3.1 Indicator-Dilution Method

A bolus of tracer is rapidly injected into the vessel, and the variation in downstream concentration of the tracer versus time is measured until the bolus has passed. The tracer will mix with a large amount of blood (Zierler, 1962). Considering that the tracer is introduced at Voxel 0 (refer to Fig. 4), it must leave the system at Voxel. All the flow that is passing through Voxel came from Voxel 0. It is assumed also that there is no recirculation. Considering $C_a(t)$ and $C_p(t)$ tracer concentrations, respectively, at Voxel 0 and Voxel, and the transfer function $h(t)$ that is the response to impulse, it is possible to write

$$C_p(t) = C_a(t) * h(t) \quad (2)$$

where the $*$ indicates convolution.

3.2 γ Variate Model

Ignoring the blood recirculation influence, the tracer concentration can be fitted by a γ function

$$\gamma(t) = a(t - b)^c \exp\left(-\frac{t - b}{d}\right) \quad (3)$$

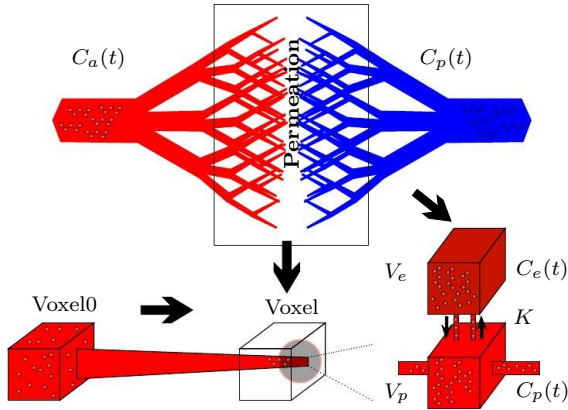


Fig. 4. A simplified two-compartment model for exchange of tracer in tissue between a vascular volume and an extravascular volume ($c_p(t)$ represents the blood plasma tracer concentration and $c_e(t)$ represents the extravascular extracellular tracer concentration).

where $t \geq b$, and a, b, c and d are constants (Brands et al., 2011). Considering that the transfer function $h(t)$ is a γ function and using (2) it is possible to determine constants a, b, c and d .

The γ fit model simplifies the analysis of perfusion considering the peak tissue concentration during the initial transit after a bolus injection. However, this will directly reflect perfusion only if the entry of tracer is completed prior to any loss of tracer in the veins. This condition will not be met in general, especially with more rapid flow rates (Axel, 1995).

3.3 The Proposed New Perfusion Model

In this work, it is proposed a method that combines the robustness to signal distortion from the γ fitting model and the tissue permeation from the two compartment model (McGrath et al., 2009). By assuming that no contrast agent escapes from the vascular flow, the γ fitting model is conventionally used to avoid the influence of noise and recirculation. The two compartment model, on the other hand, takes into account the permeation out of the blood vessels.

The method proposed here exclusively considers as input and output the data obtained from the MR temporal sequence of images, and the γ function is assumed to be the response to the impulse. The intravascular blood concentration in Voxel is assumed to be represented by a γ variate model, $C_p(t) = C_a(t) * \gamma(t)$. According to Fig. 4, the permeation out of the vessel at Voxel is estimated by the two compartment model (Axel, 1995) as

$$V_e \frac{dC_e(t)}{dt} = K(C_p(t) - C_e(t)) \quad (4)$$

where V_e is the blood volume that permeates out of the vessel, $C_p(t)$ is the tracer concentration inside the vessel and $C_e(t)$ is the tracer concentration that permeates out of the vessel. K is a transfer coefficient. Considering the initial condition $C_e(0) = 0$, then

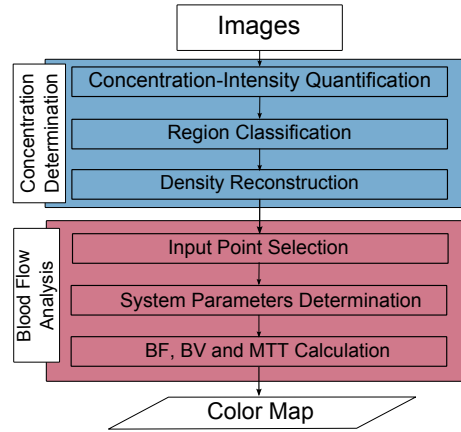


Fig. 5. Outline of the proposed method.

$$C_e(t) = \frac{K}{V_e} \int_0^t C_p(t') \exp\left(-K \frac{t-t'}{V_e}\right) dt'. \quad (5)$$

Concentration of tracer $C_t(t)$ at Voxel, is given by

$$C_t(t) = \frac{V_p C_p(t) + V_e C_e(t)}{V_p + V_e} \quad (6)$$

$$= v_p C_p(t) + \kappa \int_0^t C_p(t') \exp\left(-\kappa \frac{t-t'}{v_e}\right) dt'$$

where v_e is the intravascular volume, and

$$v_e = \frac{V_e}{V_p + V_e}, \kappa = \frac{K}{V_p + V_e} \quad (7)$$

v_e ($v_p = 1 - v_e$) and κ as well the parameters of the γ function can be determined by fitting $C_t(t)$ to the measured response curve. Other pulmonary perfusion indexes blood volume and MTT are given by

$$BV = \frac{\int_0^\infty C_p(t) dt}{\int_0^\infty C_a(t) dt}, \quad MTT = \frac{\int_0^\infty t \gamma(t) dt}{\int_0^\infty \gamma(t) dt} \quad (8)$$

After some manipulation, (8) can be simplified to

$$MTT = d(c + 1) + b, \quad (9)$$

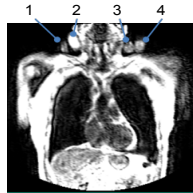
where b, c and d are parameters from (3). BF is determined by BV/MTT .

Figure 5 shows the outline of the proposed method. The concentration determination block has three steps: concentration intensity quantification (explained in section 2), region classification and density reconstruction. The lung and the heart boundaries are manually determined in the region classification. The density reconstruction is performed by using the determined concentration \times pixel intensity mapping at the heart and lung pixel regions. The input function is determined by selecting a point at the pulmonary artery. The system parameters are determined using the proposed perfusion model.

Table 1. Subject characterization

Subject	gender	Slice	Age	Injure
A	Male	10 th	60 ~ 70	cancer
B	Male	10 th	80 ~ 90	cancer
C	Female	2 nd	70 ~ 80	lung adenoma
D	Female	3 rd	40 ~ 50	lung adenoma
E	Female	2 nd	40 ~ 50	lung adenoma
F	Male	0 th	70 ~ 80	pericardial cyst
G	Female	1 st	60 ~ 70	pericardial cyst

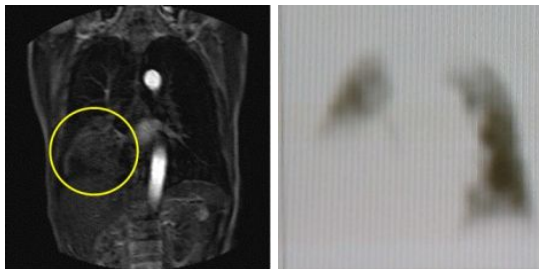
Number	Conc. [mmol/ml]
1	0.000000
2	0.000467
3	0.000239
4	0.000145



(a)

(b)

Fig. 6. (a) Phantom tracer concentration. (b) Phantom positions.



(a)

(b)

Fig. 7. (a) The original 10th slice with the tumor region. The region with cancer is shown with the yellow circle. (b) Perfusion scintigram.

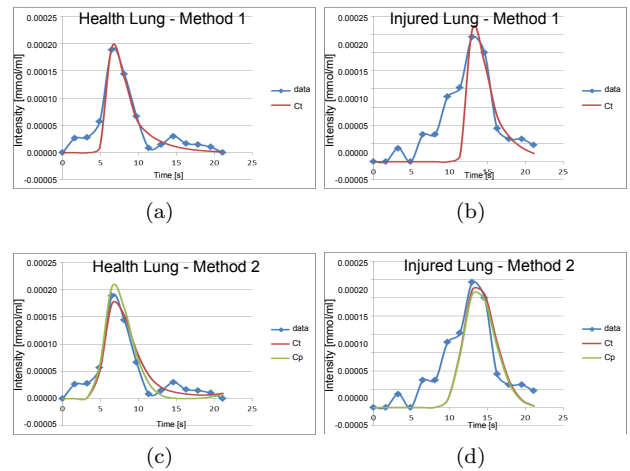
4. MATERIALS AND METHODS

The sequences of MR images⁷ were obtained from seven subjects lying supine inside a 1.5 T (Philips Medical Systems), using the gradient echo sequence method. 12 slices on 16 frames totaling 192 images acquired with a 1.54 s interval per frame, slice thickness of 12 mm, matrix size of 256 × 256 pixels and 12 bits per pixel. 5 ml of Gd tracer was injected with a concentration of 0.5 mmol/ml and speed of 6 ml/s. The images were obtained in a breath hold state. Table 1 shows some characterization of the subjects. Fig. 6(a) shows the used phantoms tracer concentrations for all subjects, and Fig. 6(b) shows the phantom positions.

5. EXPERIMENTAL RESULTS AND DISCUSSIONS

Considering subject A, Fig. 7(b) shows a scintigram and there is good agreement with the MR image shown in Fig. 7(a). First, select a position internal to the pulmonary artery and $C_a(t)$ is determined. In the following, the lung contour is determined and all voxels internal to the lung are processed using the proposed model and the

⁷ The protocol was approved by the hospital medical-ethics committee of Kanagawa Cardiovascular Respiratory Center, and informed consent was obtained from the patients.



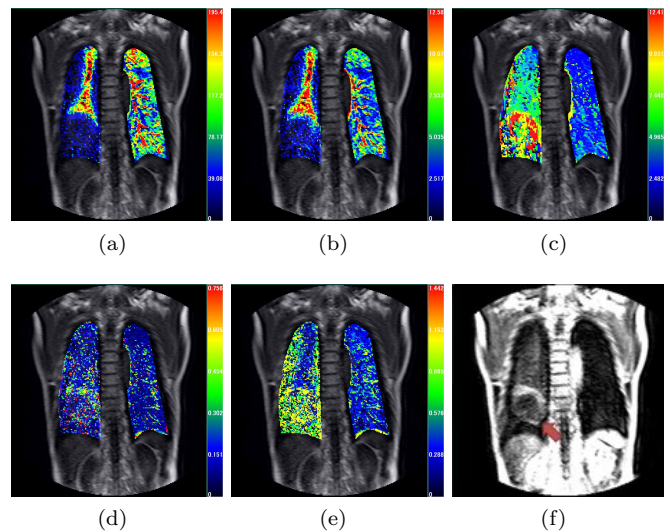
(a)

(b)

(c)

(d)

Fig. 8. Comparison of the two compartment model (method 1) and the proposed model (method 2). (a) and (c) represent a pixel selected from the healthy lung. (b) and (d) represent a pixel selected from the tumor area. The data points represent the raw observed data, the C_t (red line) represents the contrast concentration $C_t(t)$ over the complete voxel, and C_p (green line) represents the contrast concentration inside the vessels that are inside the voxel, $C_p(t)$.



(a)

(b)

(c)

(d)

(e)

(f)

Fig. 9. Subject A. (a) BF , (b) BV , (c) MTT , (d) κ , (e) v_e . (f) cancer position.

blood flow is calculated. Using $C_a(t)$ and expressions (2), (3) and (6), the contrast concentration $C_t(t)$ internal to the voxel is calculated. The curve $\gamma(t)$ is fitted by minimizing the error between the observed raw data and $C_t(t)$ at each voxel. The used minimization algorithm is the Levenberg-Marquardt. Then, two pixels are selected, one from the healthy lung (see Figs. 8(a) and (c)) and another from the tumor area (see Figs. 8(b) and (d)). The two compartment model and the proposed model are compared and the results are shown in Fig. 8. The proposed method, within the selected pixels, shows a similar result with the two compartment model. However, the proposed new method enables the determination of concepts related to the intravascular γ fitting model (see Figs. 9(a)-(c)). Figs. 9(a)-(e) shows the obtained results

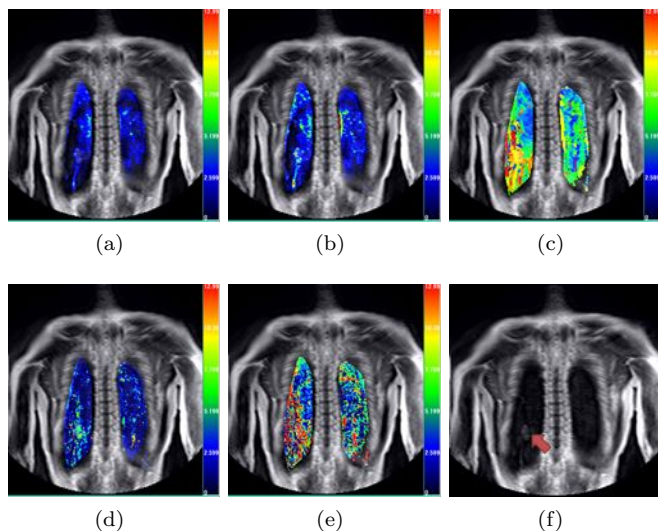


Fig. 10. Subject B. (a) BF , (b) BV , (c) MTT , (d) κ , (e) v_e , (f) cancer position.

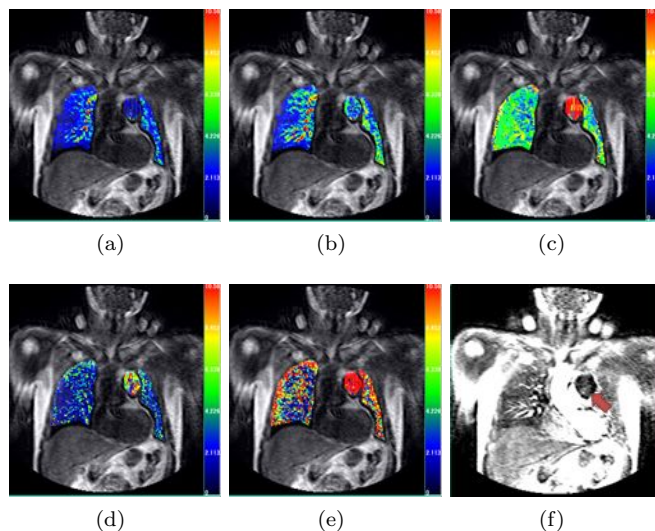


Fig. 12. Subject D. (a) BF , (b) BV , (c) MTT , (d) κ , (e) v_e , (f) lung adenoma position.

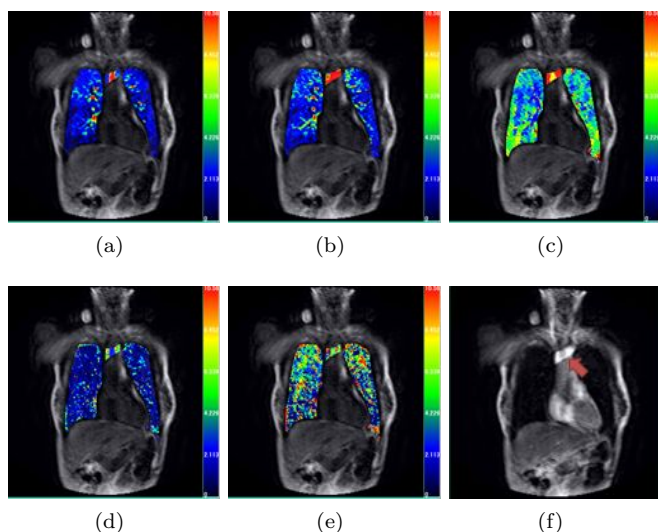


Fig. 11. Subject C. (a) BF , (b) BV , (c) MTT , (d) κ , (e) v_e , (f) lung adenoma position.

using a color map, where red represents larger values and blue smaller values. One can observe that permeation is present in both lungs (healthy and injured), but it is more intense in the injured lung (see Figs. 9(d) and (e)). Fig. 9(f) shows the image before calculations and the arrow indicates the lung cancer position.

Figures 10-15(a)-(e) show examples of the calculation results for each slice which contains lesioned region for subjects B, C, D, E, F, and G. Figs. 10-15(d)-(e) respectively show images for κ and v_e . These images show higher intensities for v_e at the lesioned region, thus permeation is an intensive phenomenon. Therefore, the tracer is accumulated in this tissue and consequently, MTT is extended (see Figs. 10-15(c)). The average value for the right lung, left lung and lesioned region is calculated and shown in Table 2. Independent of the slice, almost for all subjects the MTT is larger for the tumor region (see Figs. 10-14(c)).

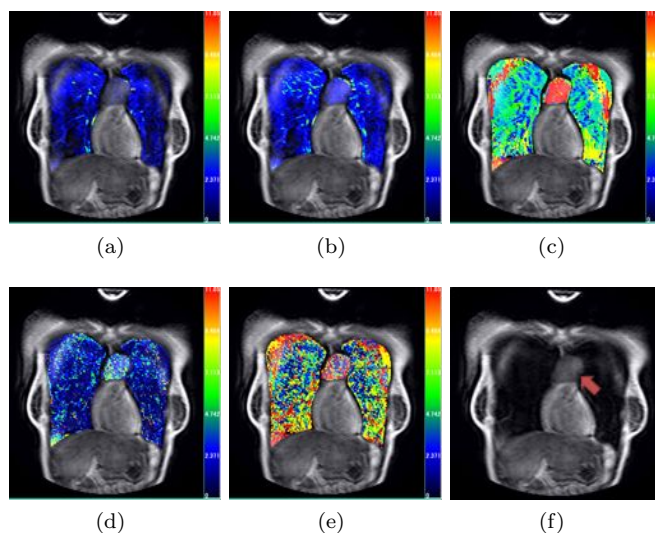


Fig. 13. Subject E. (a) BF , (b) BV , (c) MTT , (d) κ , (e) v_e , (f) lung adenoma position.

The conventional method of fitting input and output by a γ function ignores the influence of the systemic circulation. However, the Gd contrast bolus injection is not necessarily always instantaneous, thus it is impossible to assume that the signal intensity has the shape of a γ function in the pulmonary artery. The proposed method uses the observed input and output signals and assumes that the γ function with response to impulse can model the perfusion, and consequently the influence of systemic circulation is ignored. Further, since the MTT reflects the magnitude of the circulation through the aorta, it is possible to observe that, under the considered cases, the perfusion in the tumor comes mainly from the pulmonary artery. However, a small perfusion can be observed as a consequence of systemic circulation (see Figs. 8(b) and (d)).

6. CONCLUSIONS AND FUTURE WORK

In this work, a new concentration quantification method that allowed the correct observation of higher Gd concen-

Table 2. Parameters mean values. BF : [ml/100ml/min], BV : [ml/100ml], MTT : [s], κ : [1/min], LL = Left Lung, RL = Right Lung, I = Injured Region

Case		BF	BV	MTT	κ	v_e [-]
Fig. 9	LL	81.49	4.99	4.29	0.13	0.33
	RL	34.94	3.25	5.97	0.16	0.43
	I	16.66	2.60	9.37	0.21	0.51
Fig. 10	LL	29.40	2.56	5.65	0.11	0.34
	RL	32.64	2.79	7.14	0.13	0.43
	I	39.67	6.00	9.66	0.28	0.58
Fig. 11	LL	46.99	3.29	4.99	0.12	0.33
	RL	61.57	3.72	4.40	0.12	0.32
	I	177.58	30.51	12.83	0.37	0.45
Fig. 12	LL	79.61	6.40	5.31	0.19	0.61
	RL	70.68	5.30	4.98	0.16	0.44
	I	31.71	5.29	11.35	0.49	0.89
Fig. 13	LL	27.49	2.37	6.69	0.13	0.49
	RL	31.30	2.51	6.04	0.15	0.52
	I	12.88	2.32	13.36	0.26	0.55
Fig. 14	LL	9.80	1.26	7.97	0.15	0.36
	RL	10.46	1.05	7.19	0.14	0.45
	I	3.73	0.30	8.95	0.18	0.64
Fig. 15	LL	45.02	4.59	6.86	0.17	0.74
	RL	18.26	1.79	8.92	0.10	0.89
	I	34.41	4.41	8.49	0.18	0.69

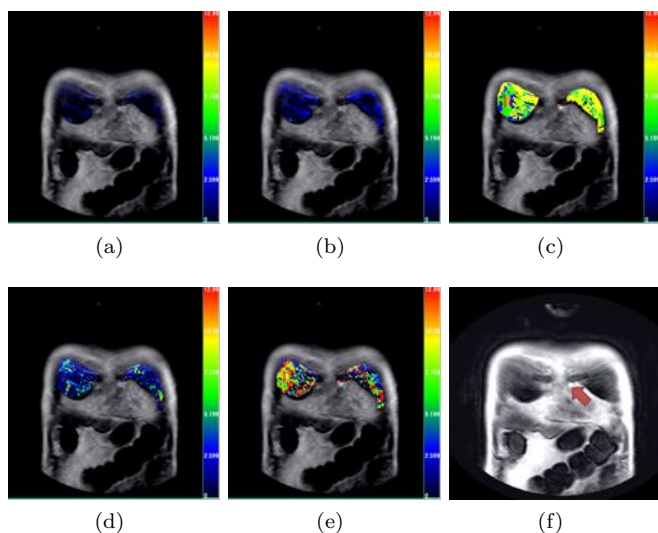


Fig. 14. Subject F. (a) BF , (b) BV , (c) MTT , (d) κ , (e) v_e , (f) pericardial cyst.

tration in the lung is proposed. Additionally, the proposed new perfusion model showed compatible results when comparing healthy and injured regions. An improved perfusion model that considers the systemic circulation is left as future work.

ACKNOWLEDGEMENTS

We are indebted to all patients and all the residents working in our units during the study period for their dedication and collaboration in providing care to the patients that participated in this research.

REFERENCES

Axel, L. (1995). Methods using blood pool tracers. In D.L. Bihan (ed.), *Diffusion and magnetic resonance perfusion*

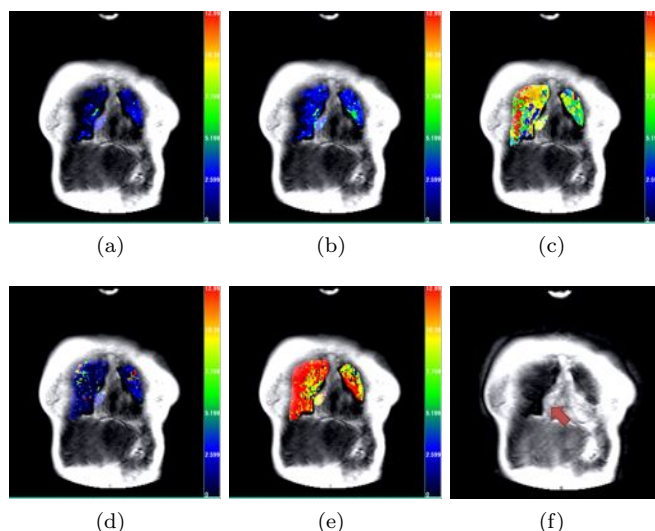


Fig. 15. Subject G. (a) BF , (b) BV , (c) MTT , (d) κ , (e) v_e , (f) pericardial cyst.

imaging, 205–211. Raven Press, New York.

Berthezine, Y., Croisille, P., Wiart, M., Howarth, N., Houzard, C., Faure, O., Douek, P., Amiel, M., and Revel, D. (1999). Prospective comparison of MR lung perfusion and lung scintigraphy. *J Magn Reson Im*, 9(1), 61–68.

Brands, J., Vink, H., and Teeffelen, J.W.G.E.V. (2011). Comparison of four mathematical models to analyze indicator-dilution curves in the coronary circulation. *Med Biol Eng Comput*, 49, 1471–1479.

Low, R.N., Sebrechts, C.P., Politoske, D.A., Bennett, M.T., Flores, S., Snyder, R.J., and Pressman, J.H. (2002). Crohn disease with endoscopic correlation: Single-shot fast spin-echo and gadolinium-enhanced fat-suppressed spoiled gradient-echo mr imaging. *Radiology*, 222(3), 652–660.

Marquardt, D. (1963). An algorithm for least-squares estimation of nonlinear parameter. *SIAM J Appl Math*, 11, 431–441.

McGrath, D.M., Bradley, D.P., Tessier, J.L., Lacey, T., Taylor, C.J., and Parker, G.J. (2009). Comparison of model-based arterial input functions for dynamic contrast-enhanced MRI in tumor bearing rats. *Magn Reson Med*, 61(5), 1173–1184.

Rosen, B.R., Belliveau, J.W., Vevea, J.M., and Brady, T.J. (1990). Perfusion imaging with nmr contrast agents. *Magn Reson Med*, 14(2), 249–265.

Shahbazi-Gahrouei, D., Williams, M., and Allen, B.J. (2001). In vitro study of relationship between signal intensity and gadolinium-DTPA concentration at high magnetic field strength. *Australas Radiol*, 45(3), 298–304.

Wang, K., Schiebler, M., Francois, C., Del Rio, A., Cornejo, M., Bell, L., Korosec, F., Brittain, J., Holmes, J., and Nagle, S. (2013). Pulmonary perfusion MRI using interleaved variable density sampling and highly constrained cartesian reconstruction (hy-cr). *J Magn Reson Im*, 38(3), 751–756.

Zierler, K.L. (1962). Theoretical basis of indicator-dilution methods for measuring flow and volume. *J Appl Physiol*, 10, 393–407.